THE 2015 EDITORIAL COMMITTEE

Published by the MDI Biological Laboratory

REPORT TITLES

Comparative Biochemistry

Comparative Physiology

Comparative Pharmacology and Toxicology

Cell Biology

Ecology

Physiological Ecology

Characterization of a bile salt transport system in isolated hepatocytes from shorthorn sculpin, *Myoxocephalus scorpius*

Shi-Ying Cai[1], Supriya Kulkarni[1] Zinta Rutins[2], Meagan Currie[3] and James L. Boyer[1]
[1] Department of Internal Medicine, Yale University School of Medicine, New Haven, CT 06520
[2] College of the Atlantic, Bar Harbor, ME 04609
[3] Greely High School, Cumberland Center, ME 04021

The Na^+-dependent bile salt transport system plays an important role in hepatic uptake of bile salts in humans and rodents, but it is uncertain whether such a system exists in marine species. Here we demonstrate that isolated shorthorn sculpin hepatocytes specifically transported ^{3}H-taurocholic acid in a time-, dose- and Na^+-dependent manner with a K_m=15 μM, a much higher affinity for bile salts than in sea lamprey, suggesting that a Na^+-taurocholate cotransporting polypeptide (NTCP, SLC10A1) is expressed in sculpin liver.

Sodium (Na^+)-dependent bile salt transport system encoded by the Na^+-taurocholate cotransporting polypeptide (NTCP/Ntcp, SLC10A1/Slc10a1) plays an important role in hepatic uptake of bile salts in humans and rodents[6]. In contrast, studies using isolated hepatocytes from the marine skate and rainbow trout (two species that represent elasmobranchs and teleosts, respectively) failed to show Na^+-dependent taurocholic acid (TCA) transport activity in these cells, indicating an Ntcp ortholog may not have evolved in these species[4, 5]. However, our previous studies in hepatocytes from sea lamprey, a more primitive vertebrate, have demonstrated Na^+-dependent uptake activity for TCA, although with low affinity (K_m = 115μM), indicating that a Ntcp ortholog evolved early in vertebrate evolution[1]. These observations indicate transport specificity of Ntcp ortholog for TCA in evolutionarily primitive species may vary among species. In this report we examined whether a Na^+-dependent TCA transport system could be identified in the liver of shorthorn sculpin (*Myoxocephalus scorpius*), a marine teleost**,** hereafter referred to as sculpin.

Sculpin were procured by MDIBL and maintained in 14˚C circulating seawater tanks with a 12-hour light-dark cycle. A ll animals were anesthetized in 0.1 g/L Tricaine and sacrificed by detaching the head from the spinal cord using a sharp knife before liver removal for collagenase perfusion. Hepatocyte preparation was carried out as we have previously described[5]. Briefly, a collagenase (type VIII, 0.05% in marine teleost Ringer) perfusion was carried out through the portal vein at 15˚C for about 25 minutes. After collagenase digestion, the liver was disrupted using forceps. Hepatocytes were obtained by low-speed centrifugation with viability averaging ~75%. A ^{3}H-TCA (1 μCi/ml, 10 μM) uptake assay was performed as previously reported. Total cellular protein concentration was used to normalize radioactivity. Non-specific binding activity to cell membranes was determined by subtracting radioactivity determined at 0˚C and 0 minute uptake as background. To assess the Na^+-dependence of the transport system, NaCl in marine teleost Ringer was replaced with equal molar amounts of choline chloride or LiCl.

TCA uptake activity occurred in a time- and dose-dependent manner at 15˚C in isolated sculpin hepatocytes with V_{max} and K_m at about 80 pmol/mg protein and 15 μM, respectively (Fig 1). ^{3}H-TCA uptake in these cells was almost completely competitively inhibited by excessive amount of the bile acid taurochenodeoxycholic acid (TCDCA, 200 μM), further suggesting there is a specific bile acid transporter in hepatocytes of this species. When NaCl in the Ringer buffer was substituted with choline chloride, the transport activities were significantly reduced by 50% after both 10 min and 30 min incubations at 15˚C (Fig 2), suggesting the presence of a Na^+-dependent bile salt transporter. Interestingly, when NaCl in the Ringer was replaced with LiCl the transport activities were significantly increased (Fig 2) by more than two-fold, in contrast to transport activity of mammalian NTCP/Ntcp.

Sculpin hepatocytes demonstrated TCA uptake activity in a Na^+- and dose -dependent manner, with a K_m = 15 μM that is comparable with human NTCP (K_m = 6 μM)[3]. This suggests an Ntcp ortholog is expressed in this marine teleost and functions in a similar fashion as its mammalian orthologs. As compared to a similar transport system in sea lamprey, sculpin Ntcp demonstrated a much higher affinity for TCA (15 μM *vs.* 115 μM). The lower K_m for TCA in sculpin hepatocytes coincides with the evolution of C24 bile acids in teleosts, further suggesting that sculpin Ntcp may be the functional determinant for hepatic bile acid uptake in this species.

Interestingly, sculpin hepatocytes demonstrated enhanced uptake of TCA when Na^+ was replaced with Li^+ in the Ringer solution. This finding indicates that there are structural differences between sculpin Ntcp and its mammalian orthologs because NTCP/Ntcp in humans and rodents lost transport activity when Na^+ was replaced with Li^+. Of note, this discrepancy was described occasionally for certain other transport systems in teleosts[2]. Future studies will be needed to sequence the sculpin *Ntcp* gene and characterize its transport activity *in vitro* in transfected cells.

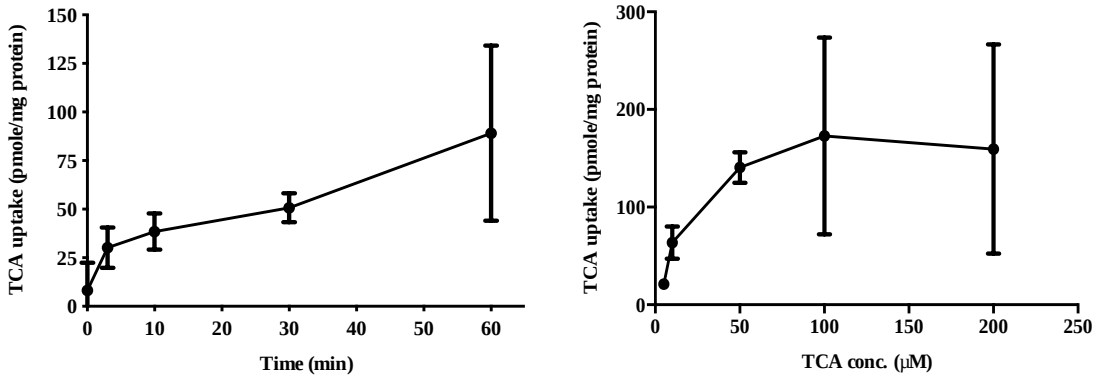

Figure 1. Isolated sculpin hepatocytes demonstrated TCA uptake activity in a time (left) and dose-dependent (right) manner at 15˚C. Michaelis-Menten analysis of TCA uptake at 15˚C for 15 minutes; n = 3-4.

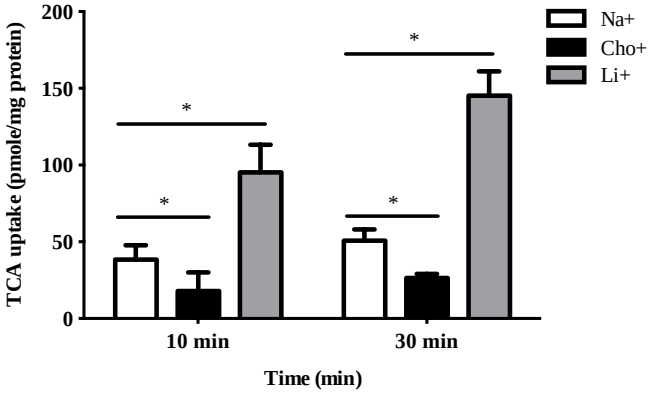

Figure 2. TCA uptake in sculpin hepatocytes is Na^+-dependent and Li^+-enhanced. $^*p < 0.05$; n = 3.

These studies were supported by National Institutes of Health Grants DK34989 and DK25636.

1. **Cai SY PA, Boyer JL.** Characterization of a bile salt transport system in isolated hepatocytes from adult sea lamprey (*Petromyzon marinus*). *Bull. Mt. Desert Isl. Biol. Lab*. 52: 20-21, 2013.
2. **Garg VK.** Effect of cations on intestinal nutrient transport in two teleosts. *Acta. Biol. Acad. Sci. Hung.* 30: 97-101, 1979.
3. **Hagenbuch B, Meier PJ.** Molecular cloning, chromosomal localization, and functional characterization of a human liver Na^+/bile acid cotransporter. *J. Clin. Invest.* 93: 1326-1331, 1994.
4. **Rabergh CM, Ziegler K, Isomaa B, Lipsky MM, Eriksson JE.** Uptake of taurocholic acid and cholic acid in isolated hepatocytes from rainbow trout. *Am. J. Physiol.* 267: G380-386, 1994.
5. **Smith DJ, Grossbard M, Gordon ER, Boyer JL.** Isolation and characterization of a polarized isolated hepatocyte preparation in the skate Raja erinacea. *J. Exp. Biol.* 241: 291-296, 1987.
6. **Stieger B.** The role of the sodium-taurocholate cotransporting polypeptide (NTCP) and of the bile salt export pump (BSEP) in physiology and pathophysiology of bile formation. *Handb. Exp. Pharmacol.* 205-259, 2011.

Further evidence for a transporter mediated urea uptake in the rectal gland of *Squalus acanthias*

Patricio Silva[1], Anya Silva[2], Milena Silva[3] and Katherine C. Spokes[4]
[1] Department of Medicine Temple University School of Medicine, Philadelphia, PA 19140
[2] Wellesley College, Wellesley, MA 02481
[3] Phillips Academy Andover, Andover, MA 01810
[4] Department of Medicine Beth Israel Deaconess Medical Center
and Harvard Medical School, Boston, MA 02215

Cartilaginous fish such as sharks, skates, and rays prevent the water from leaving their bodies by increasing the amount of solute in their tissues and body fluids. The main solute they retain is urea. The studies reported here show that the cells of the rectal gland of the shark contribute to the retention of urea by limiting the amount of urea secreted.

The concentration of urea in the plasma of the shark is 350 mM. Isolated shark rectal glands are perfused with a similar concentration of urea. The concentration of urea in the secretion of the rectal gland is very low[1]. The osmolality of the rectal gland secretion is the same as that of the plasma[1] or perfusate. Decreasing the concentration of urea in the perfusate of isolated glands decreases the concentration of salt in the secreted fluid[3], while increasing the concentration of urea in the perfusate increases the concentration of salt in the fluid[2]. During these maneuvers, the osmolality of the secretion of the rectal gland remains isotonic with the perfusate. Because of the absence of urea from the secretion of the rectal gland the concentration of salt in the secretion almost doubles. We and others have suggested that this doubling of the concentration of salt in the secretion is the result of the virtual absence of urea from the secretion. Rectal gland cells contain urea at the same concentration present in plasma or perfusate[4]. We have suggested that urea enters the rectal gland cell via a urea transporter[4]. In the present series of experiments we re-examined the effect of lowering the concentration of urea in the perfusate of isolated rectal glands and also the effect of the inhibition of the urea transporter with phloretin, on the urea content of rectal gland cells and the secretion of chloride and urea.

Isolated rectal glands of *S. acanthias* were perfused through their single artery by gravity at 16˚C and 40 mm Hg pressure with oxygenated shark Ringer's solution containing 350 mM urea and 5 mM glucose in a single-pass perfusion. Glands were stimulated with theophylline 10^{-4} M and forskolin 5 x 10^{-8} M. In the experiments with phloretin, it was added at a final concentration of 10^{-4} M after the first thirty minutes of perfusion. Venous effluent and duct fluid were collected separately from PE-90 catheters placed in the vein and duct of the gland. tCollections were made every ten minutes. At the end of each experiment, an ~100 mg piece of the rectal gland was collected, cleaned of connective tissue and frozen in liquid nitrogen for tissue urea analysis. The tissues thus collected were homogenized in 10 volumes of 100 mM phosphate buffer pH 7.6. Chloride was measured using a Buchler-Cotlove chloridometer (Labconco, Kansas City, MO). Chloride secretion was calculated from the chloride concentration in the duct fluid, the volume of the fluid, the collection time, and the weight of the gland and expressed as µEq per gram of gland per hour. The urea concentration in the dogfish blood, perfusate, rectal gland tissue homogenates, and rectal gland secretion was measured using a commercially available urea kit (QuantiChrom™ Urea Assay Kit, Hayward, CA) and expressed as mmol/l. Plasma, perfusate and rectal gland secretion osmolality were measured using a water vapor osmometer (Wescor, Logan, Utah) and reported as mOsm/l. Protein concentration in tissue homogenates was measured using Bio-Rad Protein assay (Bio-Rad Laboratories, Hercules, CA). Statistical analysis was done using Student's *t*-test and ANOVA.

Reducing the concentration of urea in the perfusate resulted in a drop in the concentration of chloride in the secretion of the gland and also in significantly lower secretion of chloride, as shown in Figure 1. As expected, the osmolality of the secretion was also significantly reduced, as shown in Figure 2. The addition of phloretin to the perfusate also resulted in a reduction of the concentration of chloride in the secretion of the gland. This reduced concentration of chloride was associated with a drop in the amount of chloride secreted. However, there was no change in the osmolality of the rectal gland secretion as compared with that of control.

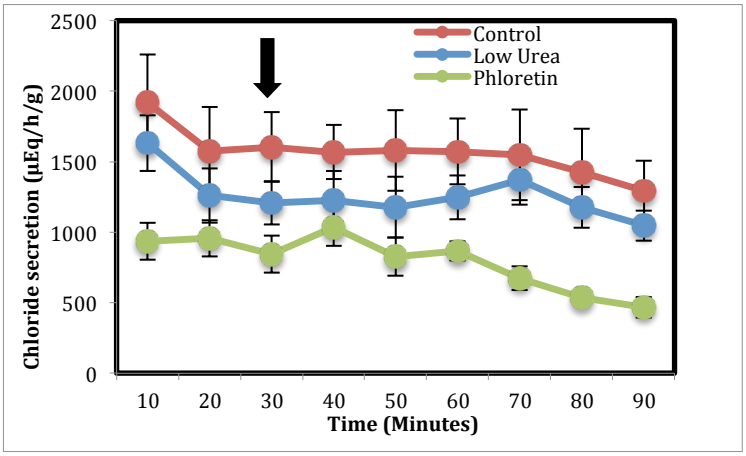

Figure 1. Effect of reducing urea in the perfusate and phloretin on the secretion of chloride by the rectal gland. Reducing the urea concentration in the perfusate to half 175 mM, caused a significant reduction in the secretion of chloride, $p < 0.001$ by ANOVA. Phloretin, 10^{-4} M added at the time indicated by the arrow also caused a significant reduction in the secretion of chloride, $p < 0.001$ by ANOVA. Data are expressed as mean ± SEM. N = 6 for all experiments.

The secretion of urea by these glands is shown in Figure 3. There was very little secretion of urea in the control gland perfused with 350 mM urea. Halving the urea concentration of the perfusate reduced the excretion of urea by the gland by approximately 27%, a statistical significant decrease by ANOVA, The addition of phloretin resulted in a progressive and significant increase in the amount of urea in the secretion of the gland as shown in the figure.

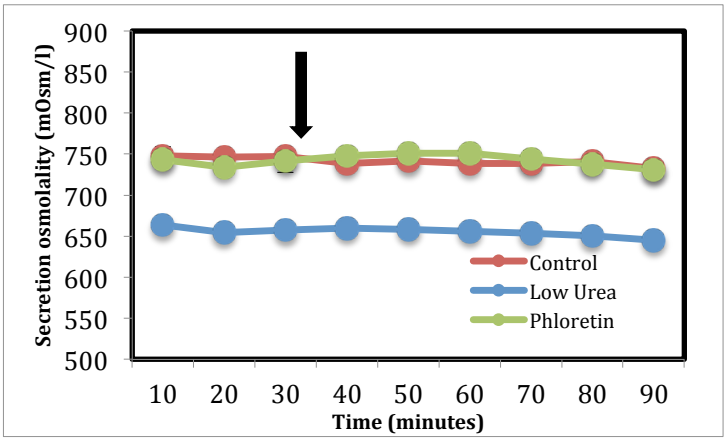

Figure 2. Effect of reducing urea in the perfusate on the osmolality of the rectal gland secretion. Halving the urea concentration the perfusate reduced significantly the osmolality of the secretion, $p < 0.001$ by ANOVA. Phloretin, 10^{-4} M added at the time indicated by the arrow, had no effect on the osmolality of the secretion. Points are mean ± SEM. Measures of dispersion cannot be seen because they are smaller than the symbols. N = 6 for all experiments.

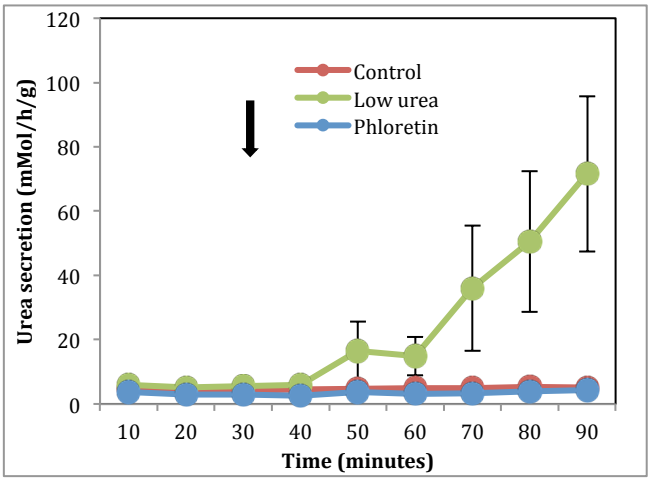

Figure 3. Effect of reducing the concentration of urea in the perfusate and phloretin on the secretion of urea by isolated perfused rectal glands. The secretion of urea that was low in the control experiments was further reduced by decreasing the concentration of urea in the perfusate to 175 mM, $p < 0.025$ by ANOVA. Phloretin 10^{-4} M added at the time indicated by the arrow, caused an unexpected rise in the urea secretion by the gland, $p < 0.0001$ by ANOVA. Points are mean ± SEM. Measures of dispersion cannot be seen in all the series because they are smaller than the symbols. N = 6 for all experiments.

The intracellular concentration of urea is shown in Figure 4. In the glands perfused with half the usual concentration of urea there was significant drop in its intracellular concentration to 32% of that seen in the glands perfused with 350 mM. Perfusions with phloretin, in the presence of 350 mM urea also resulted in a reduction of he intracellular concentration of urea to 62% of the control glands perfused with 350 mM urea.

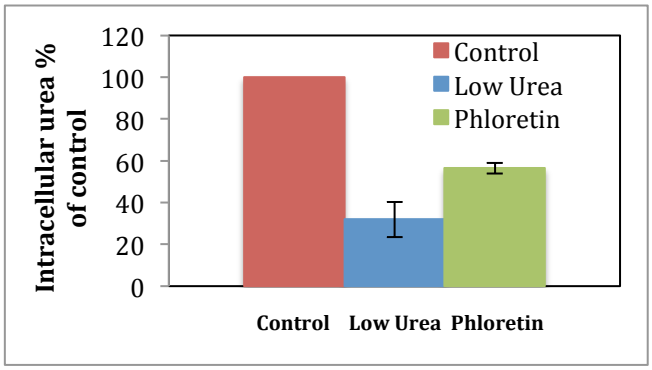

Figure 4. Effect of reducing the urea concentration in the perfusate of isolated perfused rectal glands and of phloretin on the intracellular urea concentration. Cutting in half the urea concentration of the perfsate reduced the intracellular urea concentration to 32% of control, $p < 0.001$ by Student's *t*-test. Phloretin, 10^{-4} M, significantly reduced the intracellular concentration of urea, $p< 0.001$ by Student's *t*-test. Columns are mean ± SEM. N = 6 for control and low urea and 4 for the phloretin experiments.

The observation that reducing the urea concentration in the perfusate of the isolated glands decreases the osmolality and the concentration of chloride of the secretion confirms pervious observations, and supports the notion that urea plays a role in the secretion of salt by the rectal gland. The fact that urea is present in only small amounts in the secretion of the gland that is isotonic with the plasma, allows the concentration of chloride to rise in the secretion and thus increase the total amount of salt excreted.

We have previously shown that rectal gland cells contain urea at the same concentration as that in the plasma or perfusate. Phloretin, an inhibitor of urea transporters, reduced the intracellular urea concentration of the rectal gland cells, as shown here. This observation suggests that the uptake of urea by the cells is mediated by a urea transporter present in the cell membrane. The functional effects of phloretin are also of interest. Sixty minutes after starting the perfusion of the gland with phloretin, the concentration of chloride in the perfusate dropped by 20%. In association with the drop in the concentration of chloride, the total secretion of chloride also dropped. These observations support the concept that urea, present in the plasma and the rectal gland cells, but not in the secretion of the rectal gland cells, allow the concentration of chloride in the secretion to be higher than that in the plasma. An interesting observation, yet unexplained, is that phloretin increases the concentration of urea in the secretion of the rectal gland. This unexplained phenomenon has been reported in another epithelia, the gills of the *S. acanthias*.[2]

1. **Burger JW, Hess WN.** Function of the Rectal Gland in the Spiny Dogfish. *Science.* 131: 670-671, 1960.
2. **Pärt P, Wright PA, Wood CM.** Urea and water permeability in dogfish (*Squalus acanthias*) gills. *Comparative Biochemistry and Physiology Part a, Molecular & Integrative Physiology*, 119, 117–123, 1998.
3. **Silva P, Stoff JS, Solomon RJ, Rosa R, Stevens A, Epstein J**. Oxygen cost of chloride transport in perfused rectal gland of *Squalus acanthias*. *J. Membr. Biol.* 53: 215-221, 1980.
4. **Silva P, Spokes KC, Kinne R.** The intracellular concentration of urea in the rectal gland of *Squalus acanthias. Bull. Mt. Desert Isl. Biol. Lab.* 52:15-17, 2013.

Identification and quantification of gene expression during angiogenesis in the skate, *Leucoraja erinacea*

Jacob C. Bruce[1], Eve Galen[2], Benjamin King[3], Bram V. Lutton[4]
[1] Southern Maine Community College, South Portland, ME 04106
[2] The Brearly School, New York, NY 10028
[3] Mount Desert Island Biological Laboratory, Salisbury Cove, ME 04672
[4] Endicott College, Beverly, MA 01915

The skate, *Leucoraja erinacea*, provides a unique model for studies of hematopoiesis (blood cell production and differentiation) and angiogenesis (formation of new blood vessels). These animals lack bone, allowing easier access to unique and less complex hematopoietic stem cell niches; moreover, they undergo extensive angiogenesis during their reproductive cycles, thereby potentially providing novel insight into the importance of vascular niches. This study further demonstrates the comparability between mammalian and elasmobranch hematopoietic stem cell activity and begins to quantify changes in gene expression during periods of increased angiogenesis and cellular mobilization.

Bone marrow, the tissue responsible for hemopoiesis in mammals, is comprised of vascular and endosteal niches[5]. *L. erinacea* and other elasmobranchs (sharks, skates and rays) have cartilaginous skeletons, *i.e.*, no endosteum, and thus, house hematopoietic stem cells (HSCs) within only a vascular niche. The epigonal organ (EO) of the skate, a homolog of mammalian bone marrow in direct cellular and vascular contact with the gonads, shows a significant increase in cellular turnover (proliferation and apoptosis), as well as angiogenesis, when females transition into reproductive activity[2,3,4]. These interactions between primary immune tissue and primary reproductive organs in *L. erinacea* suggests further study of these neuroendocrine-immune relationships may provide novel insight into the cellular and genetic mechanisms of hematopoiesis and angiogenesis.

In 2012, our lab observed chemokine receptor 4 (CXCR4) expression in the EO of *L. erinacea*, suggesting homologous molecules are involved in chemokine signaling between elasmobranchs and mammals. While they are known to be pleiotropic molecules, CXCR4 and CXCL12 are key regulators in the retention of HSCs in the bone marrow of mammals[5,6]. In 2013, *L. erinacea*-specific primers for a number of genes with hematopoietic and angiogenic effects were designed using newly developed databases with genomic and transcriptomic information, and the expression of CXCR4's cognate ligand, CXCL12, was observed in the EO[1].

The goals of the current experiment were to demonstrate additional genes, as well as to assess the expression levels of genes in *L. erinacea* that are homologous to genes with known hematopoietic and angiogenic functions in mammalian bone marrow. Once identified, we aimed to quantify the change in expression of these genes between non-reproductively active (NRA) and reproductively active (RA) states. Standard PCR was used to demonstrate the expression of VEGFR1, VEGFR2, c-kit and SCF, which are receptor/ligand pairs known to play key roles in hematopoiesis and angiogenesis in mammals.[7] qPCR was then used to quantify the expression of CXCR4 and CXCL12 in ten female skates (five NRA and five RA)[1].

PCR Primers were developed for CXCR4, CXCL12, c-kit, SCF, VEGFR1, VEGFR2 genes, and β-actin (the qPCR baseline standard) using *L. erinacea* transcriptome data. The NCBI database was used to get the FASTA code for the human sequence of each gene, which was compared to the *L. erinacea* transcriptome to find a contig (an area of sequence similarity) with the best alignment score. A reciprocal cross was performed to compare with the human genome and ensure that the correct gene had been found. The PrimerQuest tool from Integrated DNA Technologies was then used to design and order primers from the contig.

In RA *L. erinacea* we observed a trend of increased CXCR4 expression and decreased CXCL12 expression compared to the NRA group, which indicates the possibility that reproductive activity plays a role in mobilization. However, possibly due to our limited sample size of ten EO tissues (from 5 animals) for each group, the data did not indicate a statistically significant difference of increasing CXCR4 expression of decreasing CXCL12 expression as hypothesized. Data for SCF, c-kit, VEGFA, VEGFR1 and VEGFR2 genes currently show no trends or significant changes in levels of expression in RA compared to NRA individuals. The interaction between CXCR4 and CXCL12 and a panel of additional genes are currently under investigation to further elucidate the role of stem cell mobilization in angiogenesis and revascularization. In continuing this work, we will increase our sample size to reduce the impact of variation among individual specimens.

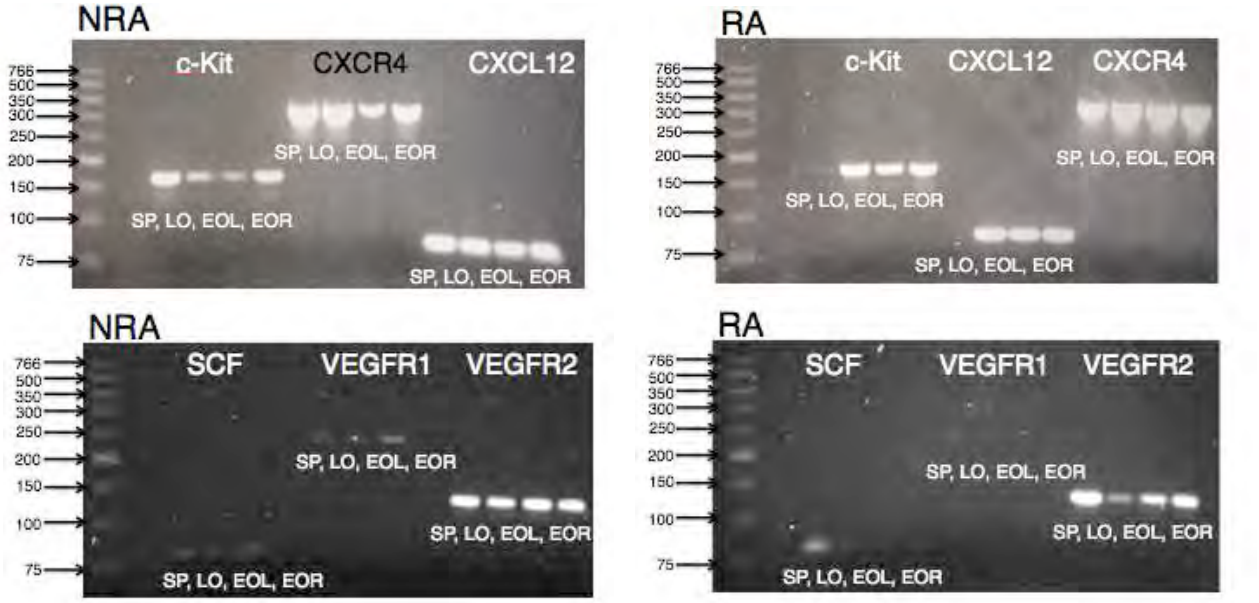

Figure 1. Representative PCR amplicons demonstrating gene expression in hematopoietic tissues of *L. erinacea.* Tissues from left (EOL) and right (EOR) epigonal organs as well as the spleen (SP) and Leydig organ (LO).

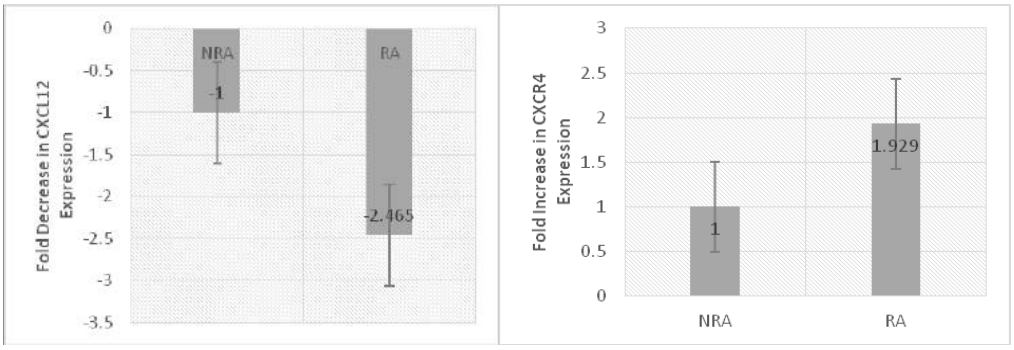

Figure 2. qPCR histogram plots depicting fold change (ratio of the initial value *versus* the final value) of gene expression from NRA to RA; positive or negative one-fold change for NRA is baseline by which RA up- or down-regulation is scaled.

This research was supported by an NSF REU grant (NSF DBI-1005003), the Salisbury Cove Research Fund, the David Evans Fellowship Fund, the Terence C. Boylan Fellowship Fund, the John W. Boylan fund, the Leon Goldstein Fund, and the James Slater Murphy, M.D., Fellowship Fund. We also acknowledge the prior contribution of Taylor Hersh and assistance of Chris Smith (MDI Biological Laboratory).

1. **Hersh T, King B, Lutton BV.** Novel bioinformatics tools for analysis of gene expression in the skate, *Leucoraja erinacea*. *Bull. MDI Biol. Lab.* 53:16-18, 2014.
2. **Lutton BV, Callard IP.** Effects of reproductive activity and sex hormones on apoptosis in the epigonal organ of the skate (*Leucoraja erinacea*). *Gen Comp Endocrinol*. 154:75-84, 2007a.
3. **Lutton BV, Callard IP.** Influence of reproductive activity, sex steroids, and seasonality on epigonal organ cellular proliferation in the skate (*Leucoraja erinacea*). *Gen Comp Endocrinol*. 155:116-125, 2007b.
4. **Lutton BV, Callard IP.** Morphological Relationships and Leukocyte Influence on Steroid Production in the Epigonal Organ-Ovary Complex of the Skate, (*Leucoraja erinacea*). *Journal of Morphology*. 269:620-629, 2008.
5. **Morrison SJ, Scadden DT**. The bone marrow niche for haematopoietic stem cells. *Nature*, 505:327-334, 2014.
6. **Tanegashima K, Suzuki K, Nakayama Y, Tsuji K, Shigenaga A, Otaka A, Hara T**. CXCL14 is a natural inhibitor of the CXCL12-CXCR4 signaling axis. *FEBS Lett*. 587:1731-175, 2013.
7. **Wilson A, Trumpp A**. Bone-marrow hematopoietic-stem-cell niches. *Nat. Rev. Immunol*. 6:93-106, 2006.

Investigation of the role of novel gene HPS3 and microRNA 636 in proteinuria on zebrafish (*Danio rerio*)

Karen M. Schaeffer[1], Heiko Schenk[1], Patricia Schroder[2], Lynne Staggs[2], Mario Schiffer[1,2], Hermann Haller[1,2]
[1] Division of Nephrology, Hannover Medical School, Carl-Neuberg-Straße 1, 30625 Hannover, Germany
[2] Mount Desert Island Biological Laboratory, Salisbury Cove, ME 04672

As part of the study of proteinuria as a key symptom of many chronic kidney diseases, the relevance of novel gene HPS3 and microRNA 636 for the glomerular filtration barrier (GFB) is investigated by injecting morpholino oligonucleotides and microRNA mimics in zebrafish larvae to cause a knockdown of HPS3 (Hermansky-Pudlak-Syndrome Gene 3) and the target genes of microRNA 636. To understand the relevance of the genes, we examined the phenotype, the fusion of glomeruli and the development of proteinuria in injected zebrafish. Thus far our results indicate that knockdown of HPS3 and overexpression of microRNA 636 effect the GFB through causing proteinuria and fish with edema.

Based on an up-regulation of the microRNA 636 in the urine of patients suffering from Alport's syndrome[1], a rare but serious kidney disease that includes proteinuria as part of a complex of severe symptoms, one could identify HPS3 as a target of miRNA[2] 636 through next generation sequencing. HPS3 is one of nine identified human HPS-causing genes[3]. We hypothesized that novel gene HPS3 and the microRNA 636 play a role in proteinuria.

To evaluate the hypothesis we injected three morpholinos[4,5] in transgenic GFB-labeled zebrafish larvae: a morpholino to knockdown HPS3, a microRNA 636 mimic and a control morpholino without binding potential to make sure not the injection process itself is harmful. In addition we used uninjected wild type to consider the egg quality. To assess the damage the absence of the genes have for the glomerular filtration barrier we did a phenotype analysis5, sorting the fish in four main categories due to edema in heart and yolk sack, after 72 hours post fertilization (hpf). The eye-fluorescence assay[5,6] after 96 hpf and 120 hpf is used to investigate the fluorescence level in the retinal vessels of the zebrafish to later be able to evaluate the condition of the filtration barrier. The used transgenic zebrafish Tg(l-fabp:DBP:EGFP) express a vitamin D binding protein fused with the enhanced green fluorescent protein (DBP-EGFP). If the filtration barrier is damaged, the fluorescence level in the retinal vessels due to the loss of DBP-GFP will be reduced comparable to the loss of human albumin in proteinuria. In addition to the phenotype- and eye-fluorescence assay we look at the blood flow after 48 hpf as a control experiment to distinguish between a potential cardiac phenotype and a phenotype based on an impaired filtration barrier. Moreover the wt1b-assay[5] can be used to control whether the glomeruli are fused and the development of the kidney was influenced by the injected morpholino. This assay is performed 48 hpf with injected transgenic wt1b-fab-fish.

The analysis of the eye-fluorescence assay reveals for both, HPS3 and microRNA 636, a significant difference of maximum fluorescence in the retinal vessels between the control fish and fish injected with the morpholino (Fig 1 and 2). The data show that the injection occurs in a loss of fluorescence due to a lower concentration of GFB in the blood. Those results confirm our considerations that the knockdown of HPS3 and overexpression of microRNA 636 can cause damage to the filtration barrier and therefore create proteinuria. With the phenotype-analysis we could show that for the microRNA 636 the extent of edema in heart and yolk sack is dose depending: the higher the injected concentration, the stronger the phenotype. Especially in the range between 5 µM and 15 µM a change of concentration has a huge impact on the phenotype. While for 5uM injected microRNA 636 mimic mostly healthy fish without edema could be observed, for a injection with 15 µM the number of fish with a very strong edema is dominating. As well for HPS3 a dose dependence could be determined. Moreover the phenotypeanalysis revealed that the knockdown of HPS3 can cause very strong developmental problems for 25 µM and 50 µM (Fig 3). Since the ratio of fish with a very distinct phenotype and fish with no phenotype differs strongly in the different experiments, further research is necessary to be able to publish reproducible data

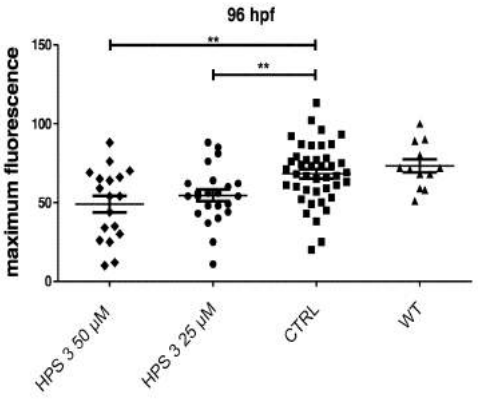

Figure 1. Analysis of the eye-fluorescence assay for HPS3. The data show a significant difference in the fluorescence level for both injected HPS3-morpholinos in comparison to the control.

for HPS3. What we could show with not only the phenotype- and eye-fluorescence assay but also our control assays is that a very high concentration has a toxic effect on the fish and causes developmental delays (seen in the wt1b-assay), the stagnation of the blood flow and a severe phenotype.

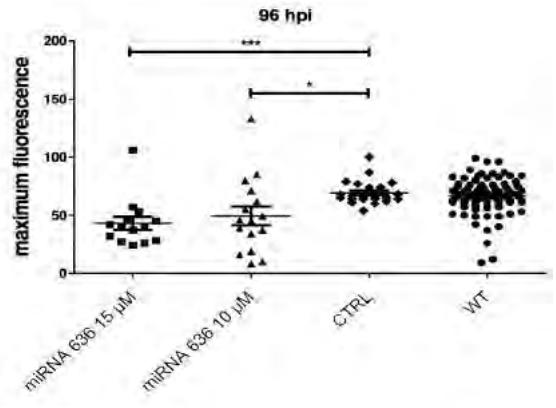

Figure 2. Analysis of the eye-fluorescence assay 96 hours post injection for microRNA 636. Fluorescence levels for the 15 µM injection and a significant difference for the 10 µM injection were significantly different than controls.

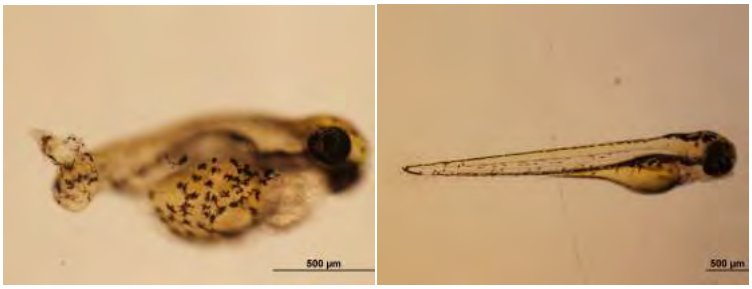

Figure 3. Phenotype-pictures for HPS3 25 µM. The left picture shows a strong phenotype for a fish that did not have blood flow after 48 hpf. The right picture shows a fish injected with the same concentration but that in comparison had blood flow after 48 hpf and does not show any edema in heart or yolk

Our next step will be to use electron microscopy to better understand the impact of the knockdown of HPS3 and overexpression of microRNA 636 on the glomerular filtration barrier. Electron microscopy enables us to understand which particular part of the glomerular filtration barrier is damaged by the absence of the genes.

This research was supported by an Institutional Development Award (IDeA) from the National Institute of General Medical Sciences of the National Institutes of Health under grant number P20GM103423 and 1P20GM104318.

1. **Savige J.** Alport syndrome: its effects on the glomerular filtration barrier and implications for future treatment. *J Physiol.* 592:4013-4023, 2014.
2. **Ha M, Kim VN.** Regulation of microRNA biogenesis. *Nat Rev Mol Cell Biol*. 15:509-524, 2014.
3. **Daly CM, Willer J, Gregg R, Gross JM.** Snow white, a zebrafish model of Hermansky-Pudlak Syndrome type 5. *Genetics*. 195:481-494, 2013.
4. **Bill BR, Petzold AM, Clark KJ, Schimmenti LA, Ekker SC.** A primer for morpholino use in zebrafish. *Zebrafish*. 6:69-77, 2009.
5. **Hanke N, Staggs L, Schroder P, Litteral J, Fleig S, Kaufeld J, Pauli C, Haller H, Schiffer M.** "Zebrafishing" for novel genes relevant to the glomerular filtration barrier. *Biomed Res Int.* 658270, 2013.
6. **Hentschel DM, Mengel M, Boehme L, Liebsch F, Albertin C, Bonventre JV, Haller H, Schiffer M.** Rapid screening of glomerular slit diaphragm integrity in larval zebrafish. *Am J Physiol Renal Physiol.* 293:F1746-750, 2007.

The function of heparanase 2 and its connection with kidney function in zebrafish (*Danio rerio*)

Heiner Riesle[1,2], Klaus Stahl[1,2], Sarah Berger[1,2], Mario Schiffer[1,2] and Hermann Haller[1,2]
[1] Hannover Medical School, Division of Nephrology, Carl-Neuberg Str.1, 30625 Hannover, Germany
[2] Mount Desert Island Biological Laboratory, Salisbury Cove, ME 04672

Heparan sulfate glycosaminoglycans are crucial components of the endothelial cell glycocalyx that constitutes together with the endothelial cells, the glomerular basement membrane and the parietal epithelial cells (podocytes) the glomerular filtration barrier in the kidney. The protein heparanase 2 was recently discovered and is speculated to regulate the activity of heparanase 1, a protein well known for cleaving heparan sulfate components of the endothelial glycocalyx. These preliminary results demonstrate that knockdown of heparanase 2 in zebrafish causes an edematous phenotype and proteinuria, probably by disrupting regulation of heparanase 1.

Heparanase 1 (HPSE1) has been studied extensively for its role in various different disease pathologies. Its physiologic function is described as an Endo-beta(1-4)-D-glucuronidase that degrades heparan sulfate polysaccharide side chains of the glycocalyx covering endothelial cells and basement membranes[1]. Several independent groups have shown in diverse animal models and humans that heparanase expression is upregulated in several primary and secondary glomerular proteinuric diseases, including diabetic nephropathy, IgA nephropathy, the heymann nephritis model (MGN) and models for MCD/FSGS, in children affected by steroid sensitive syndrome, and in anti-GBM disease[2-10]. Whereas HPSE1 has been studied extensively, little is known about the more recently discovered heparanase 2 (HPSE2) that was cloned in 2000[11]. HEPSE2 inhibits HEPSE 1 in cell culture experiments, and clinical data indicate HPSE2 expression is markedly elevated in head and neck carcinoma patients, correlating with prolonged time to disease recurrence[12,13]. However, HEPSE2 function remains to be elucidated and has not been studied in an *in vivo model*. In this study, we examined the role of HPSE2 in glomerular and vascular physiology employing a zebrafish model.

Knockdown of HPSE2 gene was performed by morpholino microinjection into 1 to 4 cell stage zebrafish embryos of a transgenic fish line (Tg l-fabp:DBP:eGFP), which produced a green fluorescence vitamin-D binding protein. These fish were compared to injected control morpholino (CTRL) and uninjected wildtype (WT) group of fish. At 72, 96 and 120 hours post-fertilization (hpf); fish were assessed for generalized edema and categorized into four subgroups: P1 (no edema) to P4 (severe edema).

Figure 1. Knockdown of HPSE2 gene causes an edematous phenotype that is not seen in WT and control fish.

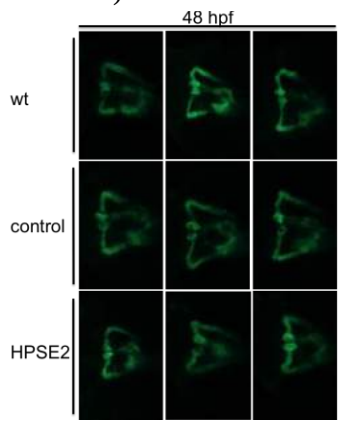

Figure 2. Glomeruli of the pronephros fuse at ~48 hpf as shown in the WT1b fish; this is not influenced by HEPSE2 knockdown.

Injection of HPSE2 morpholino resulted in development of substantial pericardial and yolk sak edema, such that most fish could be classified as P3/4 (Fig 1). In WT1b fish, regular glomerular fusion was seen at 48 hpf (Fig 2) excluding a major disturbance in early kidney development by HEPSE2 knockdown. Edema suggested loss of high molecular weight proteins from the vascular system, and loss of colloidosmotic pressure caused generalized edema. We tested this hypothesis by performing at 96 hpf and 120 hpf the fabp eye assay, which indirectly measures intravascular content of fluorescent 78 kDa high MW protein DBP in the vasculature of fish.

We observed a significant decrease in fluorescence levels in the eye as compared to wild type and control morpholino injected fish (Fig 3). There was greater loss of fluorescence at increasing morpholino

concentrations, suggesting a dose dependence of gene knockdown. These results indicated the glomerular filtration barrier is indeed compromised by HEPSE2 knockdown and that proteinuria occurs as a sequela of that.

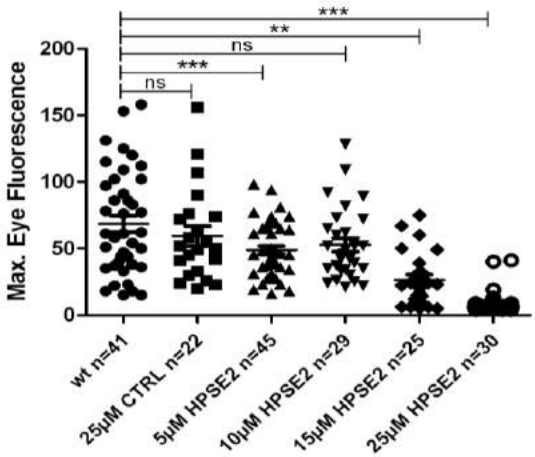

Figure 3. HPSE2 morpholino injected groups had a lower overall fluorescence level as compared to the CTRL and WT groups, indicating loss of high molecular weight plasma proteins into the urine due to damage to the glomerular filtration barrier. Loss of fluorescence was dose-dependent. $^{**}p < 0.01$, $^{***}p < 0.001$; data are mean ± SE.

These data demonstrated a significant role for HPSE2 in the structural integrity of the glomerular filtration barrier. Further experiments are needed to better understand the exact function of this novel gene and will help unravel a novel mechanism involved in causing glomerular injury and acute as well as chronic kidney disease.

This research was supported by an Institutional Development Award (IDeA) from the National Institute of General Medical Sciences of the National Institutes of Health (P20GM103423 and 1P20GM104318).

1. **Hulett MD, Freeman C, Hamdorf BJ, Baker RT, Harris MJ, Parish CR.** Cloning of mammalian heparanase, an important enzyme in tumor invasion and metastasis. *Nat Med.* 5:803-809, 1999.
2. **van den Hoven MJ, Rops AL, Vlodavsky I, Levidiotis V, Berden JH, van der Vlag J.** Heparanase in glomerular diseases. *Kidney Int.* 72:543-548, 2007.
3. **Maxhimer JB, Somenek M, Rao G, Pesce CE, Baldwin D Jr, Gattuso P, Schwartz MM, Lewis EJ, Prinz RA, Xu X.** Heparanase-1 gene expression and regulation by high glucose in renal epithelial cells: a potential role in the pathogenesis of proteinuria in diabetic patients. *Diabetes*. 54:2172-2178, 2005.
4. **van den Hoven MJ, Rops AL, Bakker MA, Aten J, Rutjes N, Roestenberg P, Goldschmeding R, Zcharia E, Vlodavsky I, van der Vlag J, Berden JH.** Increased expression of heparanase in overt diabetic nephropathy. *Kidney Int.* 70:2100-2108, 2006.
5. **Wijnhoven TJ, van den Hoven MJ, Ding H, van Kuppevelt TH, van der Vlag J, Berden JH, Prinz RA, Lewis EJ, Schwartz M, Xu X.** Heparanase induces a differential loss of heparan sulphate domains in overt diabetic nephropathy. *Diabetologia*. 51:372-382, 2008.
6. **Katz A, Van-Dijk DJ, Aingorn H, Erman A, Davies M, Darmon D, Hurvitz H, Vlodavsky I.** Involvement of human heparanase in the pathogenesis of diabetic nephropathy. *Isr Med Assoc J.* 4:996-1002, 2002.
7. **Levidiotis V, Kanellis J, Ierino FL, Power DA.** Increased expression of heparanase in puromycin aminonucleoside nephrosis. *Kidney Int.* 60:1287-1296, 2001.
8. **Kramer A, van den Hoven M, Rops A, Wijnhoven T, van den Heuvel L, Lensen J, van Kuppevelt T, van Goor H, van der Vlag J, Navis G, Berden JH.** Induction of glomerular heparanase expression in rats with adriamycin nephropathy is regulated by reactive oxygen species and the renin-angiotensin system. *J Am Soc Nephrol.* 17:2513-2520, 2006.
9. **Holt RC, Webb NJ, Ralph S, Davies J, Short CD, Brenchley PE.** Heparanase activity is dysregulated in children with steroid-sensitive nephrotic syndrome. *Kidney Int.* 67:122-129, 2005. PubMed PMID: 15610235.
10. **Szymczak M, Kuźniar J, Klinger M.** The role of heparanase in diseases of the glomeruli. *Arch Immunol Ther Exp (Warsz)*. 58:45-56, 2010.
11. **McKenzie E, Tyson K, Stamps A, Smith P, Turner P, Barry R, Hircock M, Patel S, Barry E, Stubberfield C, Terrett J, Page M.** Cloning and expression profiling of Hpa2, a novel mammalian heparanase family member. *Biochem Biophys Res Commun.* 276:1170-1177, 2000.
12. **Levy-Adam F, Feld S, Cohen-Kaplan V, Shteingauz A, Gross M, Arvatz G, Naroditsky I, Ilan N, Doweck I, Vlodavsky I.** Heparanase 2 interacts with heparan sulfate with high affinity and inhibits heparanase activity. *J Biol Chem.* 285:28010-28019, 2010.
13. **Doweck I, Kaplan-Cohen V, Naroditsky I, Sabo E, Ilan N, Vlodavsky I.** Heparanase localization and expression by head and neck cancer: correlation with tumor progression and patient survival. *Neoplasia*. 8:1055-1061, 2006.

Zn^{2+} increases multidrug resistance-associated protein 2 (Mrp2) transport activity in killifish (*Fundulus heteroclitus*) renal proximal tubules

Alexander Zaremba[1], Florian Umstätter[1, 2], David S. Miller[3], Anne Mahringer[1] and Gert Fricker[1]
[1] Institute of Pharmacy and Molecular Biotechnology, University of Heidelberg, 69120 Heidelberg, Germany
[2] Goethe University Frankfurt, 60438 Frankfurt am Main, Germany
[3] Laboratory of Signal Transduction, NIH/NIEHS, Research Triangle Park, NC 27709

One function of the vertebrate renal proximal tubule is the excretion into the urine of potentially toxic metabolites and foreign chemicals. This is accomplished through the action of numerous transport proteins located in the plasma membrane. Here we show that exposing killifish renal proximal tubules to $ZnCl_2$ rapidly and reversibly increases the activity of one such transporter, Mrp2, and that this increase is initiated through complex intracellular signaling.

Mrp2 is an ATP-driven efflux transporter that handles a wide range of metabolites, xenobiotics and xenobiotic metabolites. In renal proximal tubule, Mrp2 is localized on the luminal plasma membrane of the epithelial cells, where it can pump chemicals into the forming urine. We previously showed that exposing killifish renal tubules to $CdCl_2$ or $HgCl_2$ rapidly decreased Mrp2 transport activity, but then increased activity and transporter expression over many hours[1].

Zn is in the same group of the periodic table as Hg and Cd. It is an essential trace element and a cofactor for many enzymes. Zn deficiency affects about two billion people in developing countries and is associated with many diseases. To determine whether $ZnCl_2$ also reduced Mrp2 activity, we exposed isolated killifish renal tubules to 0.1-1 µM $ZnCl_2$ and measured transporter activity using a fluorescent substrate (Texas red), confocal imaging and image analysis [1]. The assay measured specific and concentrative accumulation of Texas red in the tubule lumens. To our surprise, $ZnCl_2$ exposure caused a rapid increase in Mrp2 transport activity; this effect was rapidly reversed when the $ZnCl_2$ was removed (Fig 1).

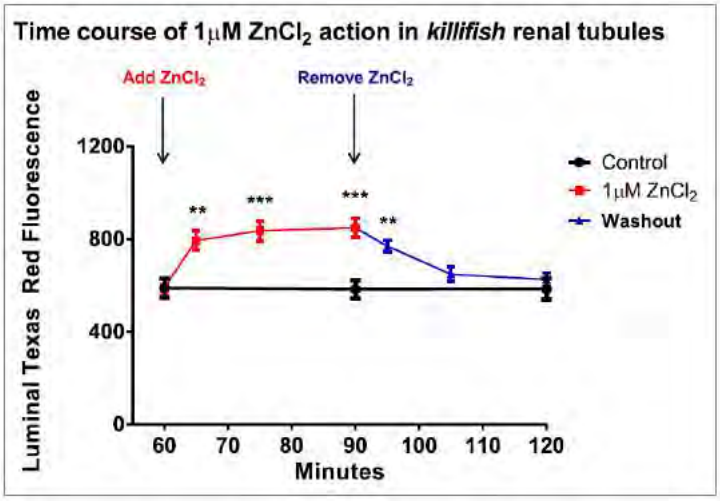

Figure 1. Time course of $ZnCl_2$ action in killifish renal tubules. Tubules were incubated to steady state with 2.5 µM Texas Red. At that time 1 µM $ZnCl_2$ was added to the medium. After 30 minutes tubules were transferred to $ZnCl_2$-free medium. Each point is the mean ± SE for 10-12 tubules from three fish. *$p < 0.05$, **$p < 0.01$, ***$p < 0.001$.

Previous studies with $CdCl_2$ indicated that *reduced* Mrp2 transport activity was signaled through endothelin receptor (ET_B), NO-synthetase (NOS) and soluble guanylyl cyclase and protein kinase C (PKC)[1]. The present experiments with specific inhibitors of each of these receptors and enzymes showed that the same processes signaled $ZnCl_2$ induced *activation* of Mrp2 transport activity.

Recent experiments with rat brain capillaries and killifish renal tubules show that signalling through phosphoinositide-3-kinase (PI3K, protein kinase B), Akt and mTOR regulates basal P-glycoprotein activity (Ref. 2 and Cannon and Miller, *unpublished data*). In the present experiments with killifish renal tubules, we also found that sphingolipid signalling to PI3K, Akt and mTOR was also involved in the Zn-driven increase in Mrp2 activity. Based on the present findings we propose a complex signaling pathway through which $ZnCl_2$

increases Mrp2 activity in killifish renal tubules (Fig 2). At present, we have no data that speak to the fact that ET_B receptor/NOS/PKC signaling is common to a Zn-driven pathway that increases Mrp2 activity and a Cd-driven pathway that decreases Mrp2 activity. Our current thinking is that the pathways diverge at PKC, with each activating a different isoform, with one leading to sphingolipid and protein kinase signaling and the other leading elsewhere.

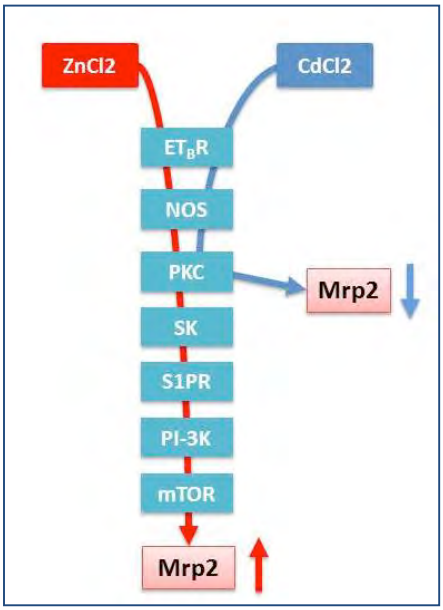

Figure 2. Signaling pathways through which $ZnCl_2$ and $CdCl_2$ regulate Mrp2 transport activity in killifish renal proximal tubules.

.

A. Zaremba was supported by Boehringer Ingelheim Fonds; F. Umstätter was supported by a David Towle fellowship.

1. **Cannon RE, Peart JC, Hawkins BT, Campos CR, Miller DS.** Targeting blood brain barrier sphingolipid signaling reduces basal P-glycoprotein activity and improves drug delivery to the brain. *Proc Natl Acad Sci USA*. 109:15930–15935, 2012.
2. **Terlouw SA, Graeff C, Smeets PH, Fricker G, Russel FG, Masereeuw R, Miller DS**. Short- and long-term influences of heavy metals on anionic drug efflux from renal proximal tubule. *J Pharmacol Exp Ther*. 301: 578-85, 2002.

Biphasic, GPER-dependent regulation of Bcrp by bisphenol A in killifish (*Fundulus heteroclitus*) renal proximal tubules

Anne Mahringer[1, 2], S. Nickel[1], Florian Umstätter[3], Alexander Zaremba[1, 2], David S. Miller[4] and Gert Fricker[1, 2]
[1] Institute of Pharmacy and Molecular Biotechnology, University of Heidelberg, 69120 Heidelberg, Germany
[2] Mount Desert Island Biological Laboratory, Salisbury Cove, ME 04672
[3] Goethe University Frankfurt, 60438 Frankfurt am Main, Germany
[4] Laboratory of Signal Transduction, NIH/NIEHS, Research Triangle Park, NC 27709

One function of the kidney is to excrete potentially toxic foreign chemicals, a process that occurs in the proximal tubule. Breast Cancer Resistance Protein (Bcrp) is an ATP-driven transport protein, expressed in proximal tubule that does just that. Here we show that bisphenol a, an environmental estrogen, regulates Bcrp activity in killifish proximal tubules through a novel mechanism involving a non-classical estrogen receptor.

Breast Cancer Resistance Protein (Bcrp) is an ATP-driven drug efflux pump that is highly expressed in barrier and excretory tissues. Estrogen regulates Bcrp expression in human placenta, breast cancer cells in culture and in rat and mouse brain capillaries. However, available evidence suggests tissue-specific modes of regulation. In addition to the hormone (estradiol, E2), persistent environmental pollutants also act through estrogen receptors to elicit estrogen-like effects. Bisphenol A (BPA) is one such environmental estrogen. It has a lower binding affinity to estrogen receptors than E2 and it exerts only a weak, genomic down-regulation of Bcrp in *rat* brain capillaries compared to E2[1,3]. However, BPA also binds to G-protein-coupled estrogen receptor 1 (GPER) at pico- to nanomolar concentrations and elicits even stronger, immediate effects than E2[1,4]. Thus, BPA is able to alter estrogenic signaling by interacting with non-classical receptors. Here we show that in killifish renal tubules BPA has a biphasic effect on Bcrp transport activity, with nanomolar concentrations reducing activity and micromolar concentrations increasing activity.

We used confocal microscopy to measure steady-state accumulation of mitoxantrone, a fluorescent Bcrp substrate, in lumens of freshly isolated renal tubules as described previously[2]. Exposure to 10 or 100 nM BPA reduced Bcrp-mediated mitoxantrone secretion into the lumen. In contrast, micromolar concentrations of BPA and of estradiol increased Bcrp transport activity. BPA exposure did not affect transport activity of P-glycoprotein or Mrp4, but did reduce Mrp2 transport activity. G1, an agonist for GPR, had a similar biphasic dose response. The GPER antagonist, G15, abolished the responses of Bcrp to nanomolar and micromolar G1 and to nanomolar BPA, indicating action through GPER. Effects of micromolar BPA were only partially reduced by G15. However, the nonspecific ER antagonist, ICI182.780, together with G15 completely abolished the BPA-mediated stimulation of Bcrp transport, indicating involvement of classical estrogen receptors. The increase in Bcrp transport activity caused by exposure to micromolar concentrations of BPA involved intracellular signaling, since it was reduced by Brefeldin A, an inhibitor of vesicular trafficking, and by H89, an inhibitor of protein kinase A, but not by a PI-kinase inhibitor.

To date, regulation of Bcrp activity has been lined to the action of classical estrogen receptors. The present results for renal proximal tubule provide evidence for a novel mechanism of Bcrp regulation through GPER and intracellular signaling.

1. **Alonso-Magdalena P, Ropero AB, Soriano S, Garcia-Arevalo M, Ripoll C, Fuentes E, Quesada I, Nadal A**. Bisphenol-A acts as a potent estrogen via non-classical estrogen triggered pathways. *Mol Cell Endocrinol.* 355: 201-207, 2012.
2. **Nickel S, Bernd A, Miller DS, Fricker G, Mahringer A.** Bisphenol-A modulates function of ABC transporters in killifish *(Fundulus heteroclitus)* renal proximal tubules. *Bull. Mt. Desert Isl. Biol. Lab.* 52:30, 2013.
3. **Nickel S , Mahringer A**. The xenoestrogens ethinylestradiol and bisphenol A regulate BCRP at the blood-brain barrier of rats. *Xenobiotica* 44: 1046-1054, 2014.
4. **Vandenberg LN, Hauser R, Marcus M, Olea N, Welshons WV**. Human exposure to bisphenol A (BPA). *Reprod Toxicol.* 24: 139-177, 2007.

Characterizing cilia in sand dollar (*Echinarachnius parma*) embryos after lithium ion treatment

Paige C. Mundy[2], Hans W. Pope[1], and Robert L. Morris[1]
[1] Department of Biology, Wheaton College, Norton, MA 02766
[2] Department of Biology, Saint Francis University, Loretta, PA 15940

Cilia are whip-like, cell surface appendages that provide locomotory and sensory capabilities throughout the animal kingdom. During early echinoid development, cilia of different types rapidly form and differentiate on different germ layers. Lithium ion treatment can perturb embryogenesis by shifting germ layer boundaries and thereby aid in characterizing cilia differentiation. Our data suggest the change in cilia phenotype seen on the surfaces of lithium ion-treated "vegetalized" embryos is due to an increase in endodermal expression and endodermal cilia formation compared to untreated embryos.

The many forms and functions of cilia in humans result in a wide array of diseases, or "ciliopathies," when cilia form abnormally. Echinoid embryos provide a valuable model for studying cilia growth and differentiation due to rapid onset of ciliogenesis and multiple cilia types that form. *Echinarachnius parma* globally express cilia on their outer surface 22 hours post-fertilization (hpf). Four hours later, at least three distinct ciliary phenotypes arise on the gastrula stage embryo, while a primitive gut invaginates into the blastocoel lumen. To study cilia of the gut, incubation of *E. parma* embryos in sea water plus 12.5 mM lithium chloride or 6 hours from 4-10 hpf "vegetalized" embryos[1] and produced embryos with exaggerated gut domains with five distinct morphological phenotypes: long endogut (63.3% of embryos), short endogut (11.9% of embryos), unconstructed exogut (1.1% of embryos), constricted exogut (1.5% of embryos), and irregular morphology (22.2% of embryos) (n = 1,449 embryos in one trial; Fig 1). We hypothesized that an exogut region would be composed of endodermal tissue, while mesodermal expression would not be affected[2]. To test this hypothesis, vegetalized embryos were immunofluorescently stained using germ layer specific antibodies (antibody 5c7 for Endo1, gift of D. McClay, Duke University) and imaged by confocal microscopy. Our data show vegetalized embryos overexpressed endoderm in the exogut region, but also throughout the embryo (Fig 1A). Vegetalized embryos that do not exhibit the classic exogut phenotype also showed increased endodermal expression (Fig 1B). Additionally, mesodermal expression was found to be unperturbed between vegetalized and wild type embryos (not shown). These data suggest that for studying cilia types, the current model of interpreting echinoderm vegetalization based on morphology must be revised to account for variance in increased endodermal expression throughout a lithium-perturbed population.

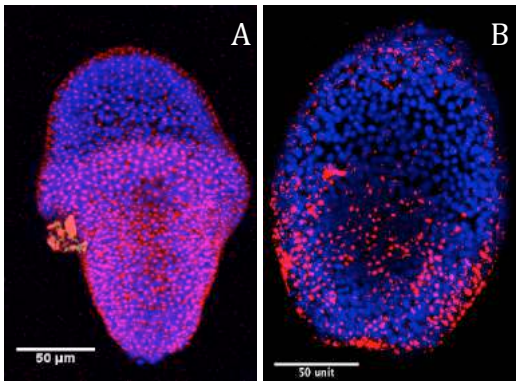

Figure 1. Endodermal expression in vegetalized *E. parma* embryos exceeds the exogut region. Two phenotypically distinct vegetalized *E. parma* embryos illustrate two of the five morphological phenotypes we observed. Blue indicates DNA and red indicates endodermal expression of Endo1. Vegetal pole is oriented downward in images. A) Vegetalized embryo with constricted exogut exhibits a classic "vegetalized phenotype" with exogut narrower than rest of embryo as seen in bottom half of image; surprisingly, Endo1 expression reveals that endoderm domain is not limited to exogut. B) Vegetalized embryo with short endogut exhibits a short invagination at vegetal pole. Endodermal expression is concentrated near the invagination, but is also seen throughout the embryo.

This research was supported by NSF REU awards from MDIBL (NSF DBI-0453391) to PCM and HWP, by an MDIBL Visiting Scientist award to RLM supported by the Salisbury Cove Research Fund and the Terence C. Boylan Fund, and by Grant #1R15HD060015-01 from the Eunice Kennedy Shriver National Institute for Child Health & Human Development, with help of the American Recovery and Reinvestment Act of 2009, to RLM.

1. **Mitsunaga K, Fujiwara A, Yoshimi T, Yasumasu I.** Stage specific effects on sea urchin embryogenesis of Zn^{2+}, Li^{+}, several inhibitors of cAMP-phosphodiesterase and inhibitors of protein synthesis. *Develop. Growth Differ.* 25: 249-260, 1983.

2. **Poustka AJ, Kühn A, Groth D, Weise V, Yaguchi S, Burke RD, Herwig R, Lehrach H, Panopoulou G.** A global view of gene expression in lithium and zinc treated sea urchin embryos: new components of gene regulatory networks. *Genome Biol.* 8:R85, 2007.

Role of genetic diversity and water quality in the 2013 decline of eelgrass (*Zostera marina*) populations of the Upper Frenchman Bay, ME coastlines

Kathleen Morrill[1], Anna Farrell[2], Alden Dirks[2,3], Mary Badger[2,4], Jane Disney[2] and Larissa Williams[1,2]
[1] Bates College, Lewiston ME 04240
[2] Mount Desert Island Biological Laboratory, Salisbury Cove, ME 04672
[3] Swarthmore College, Swarthmore, PA 19081
[4] Smith College, Northampton, MA 01063

To determine the role of genetic diversity in the 2013 loss of eelgrass (*Zostera marina*) in the upper Frenchman Bay, Mount Desert Island, a set of genetic markers were sequenced and compared against eelgrass density and tensile strength. While the genetic diversity of the eelgrass did not explain differences in health of eelgrass by site, some water quality parameters such as silica and nitrate/nitrite in the water column may be contributing factors to the decline.

Eelgrass beds (*Zostera marina*) serve a vital role invaluable to commercial supplies of seafood in Maine, by forming estuaries for young fish and shellfish. Since aerial fly-over imaging done in 1996, the coverage of eelgrass in the upper Frenchman Bay, ME, has diminished from 3,000 to less than 200 acres[1,2]. In the summer of 2013, major restoration areas around Mount Desert Island at Hadley Point, Berry Cove, and Thomas Island, established by ecologists to counter this loss, also declined. Genetic diversity of eelgrass may also explain differences in survival among populations, with higher genetic diversity potentially imparting more resistance to environmental change or physical disturbance. The genetic diversity of six populations (2 unhealthy: Berry Cove (BC) and Bar West (BW); 4 healthy: Bar East (BE), Ship Harbor (SH), Stave Island (SI), and Wonderland (W)) across Mount Desert Island was quantified using microsatellite size DNA analysis for six markers. The inbreeding coefficient (F_{IS}), a measure of genetic diversity, was calculated for each population and compared against eelgrass density; no correlation was found between the health of the site and the genetic diversity of the plants (Fig 1).

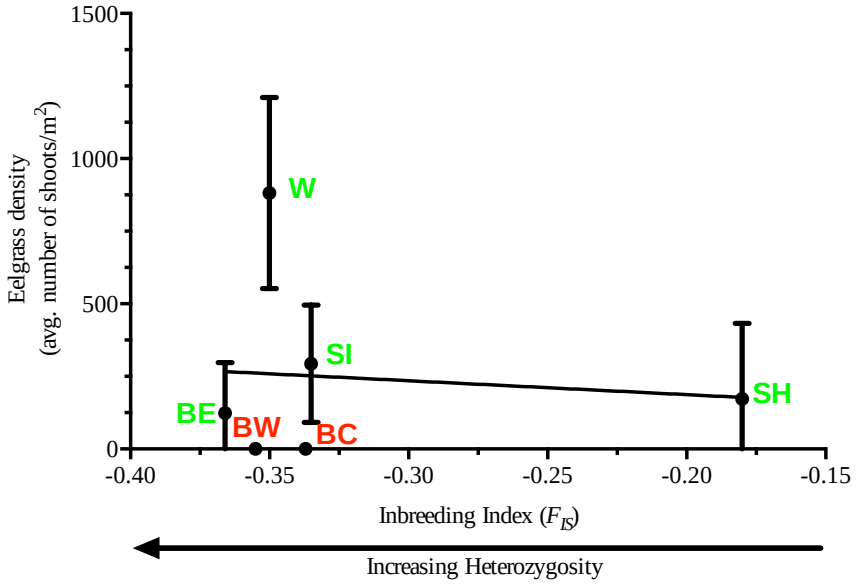

Figure 1. Linear relationship between inbreeding index (F_{IS}) and eelgrass density ($R^2 = 0.01$, $p = 0.84$). Sites in green are deemed healthy eelgrass habitats; sites in red are deemed unhealthy eelgrass habitats based on plant density.

The tensile strength of the eelgrass, perhaps a measure of resilience to physical disturbance, was compared to the genetic diversity of each site. There was no correlation found between the two variables (Fig 2), and there was no difference in healthy versus unhealthy sites in the tensile strength of the plants (Fig 3).

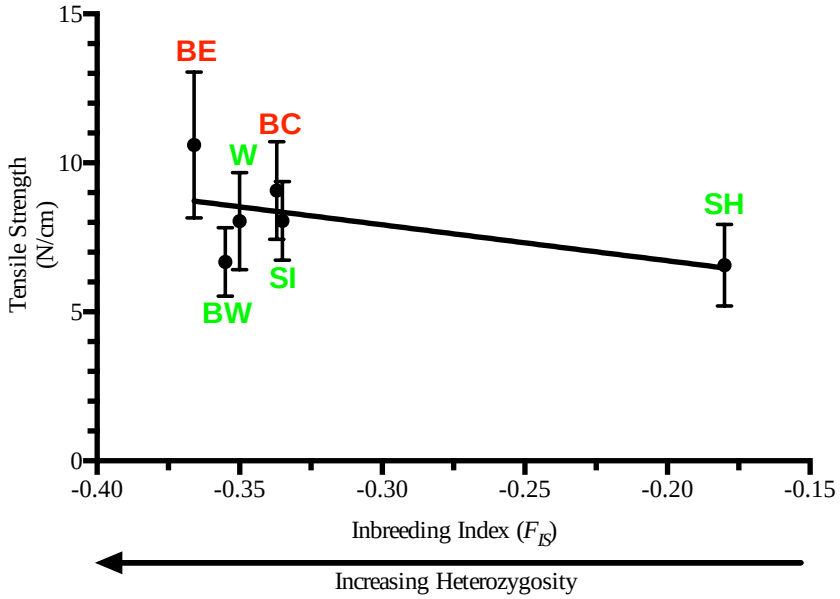

Figure 2. Linear relationship between inbreeding index (F_{IS}) and tensile strength ($R^2 = 0.31$, $p = 0.25$). Sites in green are deemed healthy eelgrass habitats; sites in red are deemed unhealthy eelgrass habitats based on plant density.

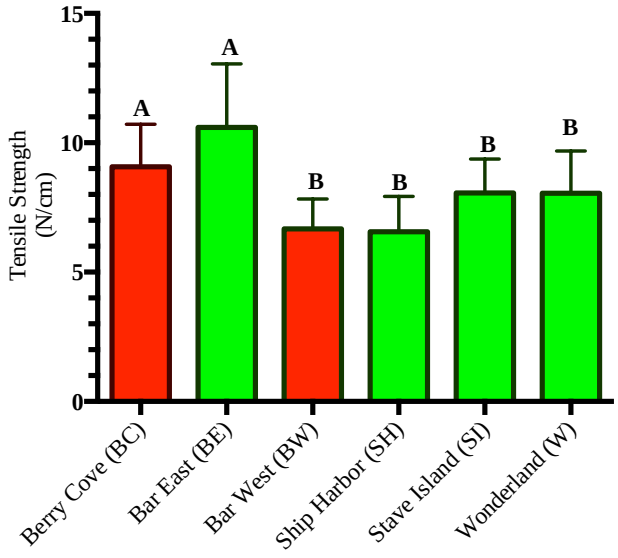

Figure 3. Average tensile strength of plants collected at healthy (green) and unhealthy sites (red). Significant differences in tensile strength was determined with a one-way ANOVA and Tukey's *posthoc* test ($\alpha = 0.05$). Letters above eelgrass habitats indicate where there were no significant difference between sites.

Genetic diversity and tensile strength did not seem to correlate with the health of eelgrass populations as was expected for Berry Cove, which had high levels of intrapopulation diversity and little differentiation from healthy sites. Nevertheless, the population at Ship Harbor, a healthy site, showed the lowest intrapopulation diversity and highest interpopulation differentiation.

To determine the role of water quality in the decline, nitrate/nitrite, ammonia, phosphorus, and silicate levels were measured using a Bran Luebbe Autoanlyzer III on four separate occasions at all sites described above, plus several additional sites, over the course of the summer. There were differences in silica in the water column among sites as determined by one-way ANOVA ($F = 2.585$, $p = 0.0125$). A comparison of all sites documented to have lost eelgrass (Jordan River, Thomas Island East, Thomas Island West, Hadley Point, Berry Cove, Lamoine Shore, and Bar West) and all sites with intact eelgrass beds (Bar East, Stave Island, Wonderland and Ship Harbor) revealed a significant difference in silica in the water column over the course of the summer (*t*-

test, $p = 0.0179$). Silica was highest where eelgrass was intact. There was also a significant difference among sites for nitrate/nitrite levels in the water column as determined by one-way ANOVA ($F = 3.00$, $p = 0.005$). A comparison of sites documented to have lost eelgrass and sites with intact eelgrass as listed above revealed a significant difference in nitrate/nitrite in the water column over the course of the summer (*t*-test, $p = 0.003$). Nitrate/nitrite levels were highest where eelgrass was intact. There was not a significant difference in ammonia levels among sites as determined by one-way ANOVA ($F = 0.780$, $p = 0.667$) and consequently, there was not a significant difference in total dissolved inorganic nitrogen (DIN) among sites ($F = 1.72$, $p = 0.099$). The same was true for phosphorus ($F = 0.385$, $p = 0.961$). The affect of water column nutrient levels on eelgrass health and susceptibility to disease and damage will be the subject of future research.

Research reported in this project was supported by an Institutional Development Award (IDeA) from the National Institute of General Medical Sciences of the National Institutes of Health under grant number P20GM103423, the Center for Regenerative Biology and Medicine at MDI Biological Laboratory (grant USAMRMC W81XWH-11-1-0425), the Bodil Schmidt-Nielsen Fund, and through NSF REU support (NSF DBI-0453391).

1. **Disney J, Thornburn L, Kiddler G.** Possible causes of eelgrass (*Zostera marina*) loss in Frenchman Bay, Maine. *Bull. Mt. Desert Isl. Biol. Lab*. 53:26-28, 2014.
2. **Bailey D, Bailey J, Kidder G, Disney J.** A citizen science approach to mapping eelgrass (*Zostera marina* L.) loss in Maine. *Bull. Mt. Desert Isl. Biol. Lab*. 53:25, 2014.

Population genetics and abundance of the invasive European green crab (*Carcinus maenas)* and its role in eelgrass (*Zostera marina*) loss around Mount Desert Island

Mary Badger[1,2], Alden Dirks[1,3], Anna Farrell[1], Jirias Charabati[1], Kathleen Morrill[4], Jane Disney[1] and Larissa Williams[1,4]

[1] Mount Desert Island Biological Laboratory, Salisbury Cove, ME 04672

[2] Smith College, Northampton, MA 01063

[3] Swarthmore College, Swarthmore, PA 19081

[4] Bates College, Lewiston ME 04240

Following the devastating 2013 loss of eelgrass (*Zostera marina*) in the upper Frenchman Bay, Mount Desert Island, the role of the invasive green crab (*Carcinus maenas*) in the decline was investigated. Neither the genetics of the crabs nor their abundance correlated to the overall health of the eelgrass. The loss of eelgrass may be due to other factors or an interplay of abiotic and biotic factors.

Zostera marina or "eelgrass" is a common seagrass found widespread in northern coastlines across the world. Eelgrass beds serve a vital role in marine ecosystems of Maine, protecting shorelines against erosive forces and providing an ecosystem for larval and juvenile fish and shellfish. Between 1996 and 2013, the coverage of eelgrass in the upper Frenchman Bay area of Mount Desert Island, ME, was reduced from 3,174 to between 75 and 183 acres[1,2]. Contrasting sites with healthy populations to sites that have sustained significant loss is key to identifying decline causation. One potential culprit in eelgrass loss is the invasive green crab (*Carcinus maenas*); green crabs voraciously target soft shell clams[3] and damage eelgrass during their foraging behavior[4, 5]. Green crabs were first introduced to the New York Harbor from Europe in the 1800s[5], and a secondary invasion of novel northern haplotypes, hypothesized to be more voracious[7], occurred in Nova Scotia during the 1980s and 1990s[3]. To determine whether the genetics or abundance of the crabs are correlative with the health of the eelgrass, crabs were assessed at seven eelgrass sites around Mount Desert Island. Using the neutral mitochondrial genetic marker, cytochrome oxidase c I (COI), the haplotype of 15 individuals per site was ascertained. Haplotype 1, the original invading haplotype, was most frequent; novel northern haplotypes (4,5,6) were found in several individuals around the island (Fig 1).

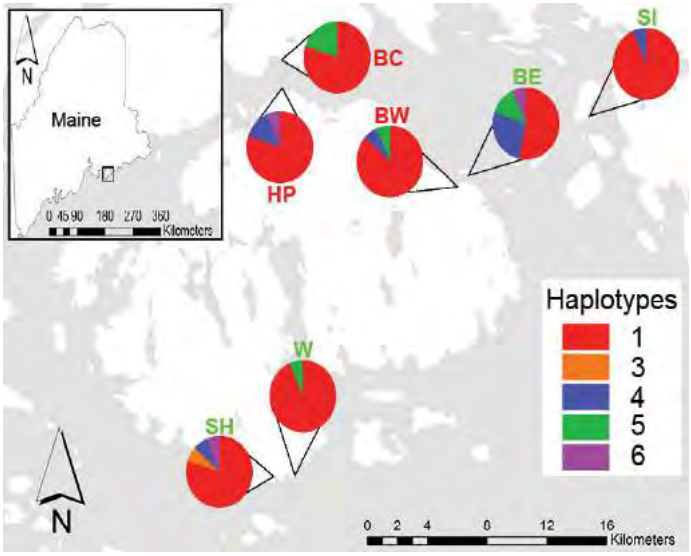

Figure 1. *C. maenas* COI haplotype frequencies per site (BC=Berry Cove; BE=Bar East; BW=Bar West; HP= Hadley Point; SH=Ship Harbor; SI= Stave Island; W=Wonderland). Sites marked in green are deemed healthy eelgrass habitats; sites in red are deemed unhealthy eelgrass habitats based on eelgrass density and biomass.

Since northern haplotypes are suspected to be more voracious, and hence cause more damage than the original invading haplotype (haplotype 1), the percent of northern haplotypes per site was compared to the health of the eelgrass, as measured by eelgrass shoot density. There was no correlation of the percent of crabs of a northern haplotype with the health of the eelgrass at that site (Fig 2).

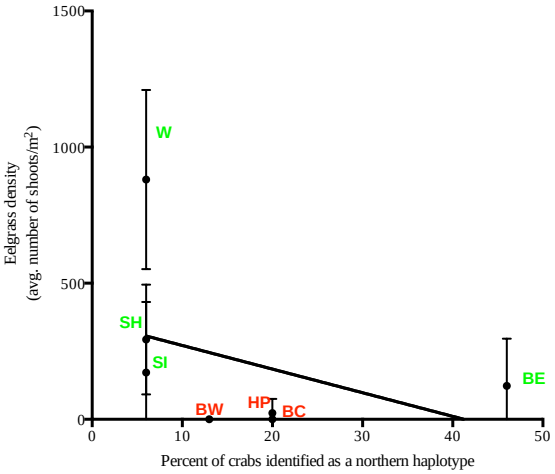

Figure 2. Linear relationship between percent of crabs identified as a northern haplotype and eelgrass density ($R^2 = 0.13$, $p = 0.38$). Sites in green are deemed healthy eelgrass habitats; sites in red are deemed unhealthy eelgrass habitats.

From green crab abundance data collected over a four-day course of sampling in September of 2014, the greatest abundances were found at Bar West, a site of considerable eelgrass loss in 2013-2014. However, green crab abundance in Berry Cove and Hadley Point, also sites of great eelgrass decline, were not significantly different from other healthy sites such as Bar East, Stave Island, and Ship Harbor (Fig 3).

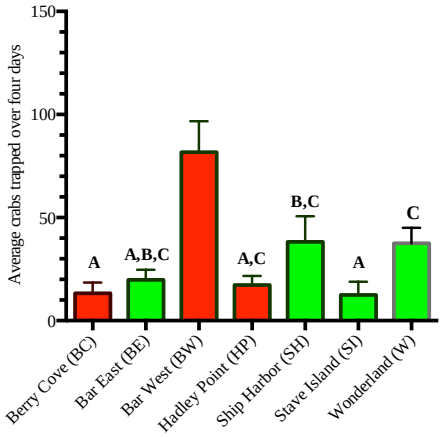

Figure 3. Average green crab (*C. maenas*) trapped over four days in September of 2014 in eelgrass habitats around Mount Desert Island. Sites in green are deemed healthy eelgrass habitats; sites in red are deemed unhealthy eelgrass habitats. Significant differences in average crabs trapped were determined with a one-way ANOVA and Tukey's *posthoc* test ($\alpha = 0.05$). Letters above eelgrass habitats indicate where there was no significant difference between sites.

While it cannot be ruled out that the presence of green crabs contributed to the 2013 eelgrass decline in Frenchman Bay, the loss of eelgrass may be due to other factors or an interplay of abiotic and biotic factors.

This project was supported by an Institutional Development Award (IDeA) from the National Institute of General Medical Sciences of the NIH (P20GM103423), the Center for Regenerative Biology and Medicine at MDI Biological Laboratory (grant USAMRMC W81XWH-11-1-0425), the Bodi Schmidt-Nielsen Fund, and through NSF REU support (NSF DBI-0453391).

1. **Disney J, Thornburn L, Kiddler G.** Possible causes of eelgrass (*Zostera marina*) loss in Frenchman Bay, Maine. *Bull. Mt. Desert Isl. Biol. Lab*. 53:26-28, 2014.
2. **Bailey D, Bailey J, Kidder G, Disney J.** A citizen science approach to mapping eelgrass (*Zostera marina* L.) loss in Maine. *Bull. Mt. Desert Isl. Biol. Lab*. 53:25, 2014.
3. **Roman J.** Diluting the founder effect: cryptic invasions expand a marine invader's range. *Proc. Biol. Sci.* 273:2453-2459, 2006.
4. **Neckles HA**. Loss of Eelgrass in Casco Bay, Maine, Linked to Green Crab Disturbance. *N Nat, in press*.
5. **Garbary D, Miller A, Williams J, Seymour N**. Drastic decline of an extensive eelgrass bed in Nova Scotia due to the activity of the invasive green crab (*Carcinus maenas*). *Mar. Biol.* 161:3-15, 2014.
6. **Compton TJ, Leathwick JR, Inglis GJ**. Thermogeography predicts the potential global range of the invasive European green crab (*Carcinus maenas*). *Div. Distr.* 16:243-255, 2010.
7. **Kanary L, Musgrave J, Tyson RC, Locke A, Lutscher F**. Modelling the dynamics of invasion and control of competing green crab genotypes. *Theor. Ecol.* 7:391-406, 2014.

A survey of developmental abnormalities in *Fundulus heteroclitus* embryos from Northeast Creek

Brent N. Lawson[1], Ari Dehn[2] and Robert L. Preston[3, 4]
[1] Southern Maine Community College, South Portland, ME 04116
[2] Ari Dehn, University of Maine at Machias, Machias, ME 04654
[3] School of Biological Sciences, Illinois State University, Normal, IL 61790
[4] Mount Desert Island Biological Laboratory, Salisbury Cove, ME 04672

The embryos of Northern killifish can develop immersed in seawater or in air when stranded on rocks or vegetation in estuaries. These embryos are remarkably tolerant to desiccation, thermal and salinity stress. About 6% of these embryos show developmental anomalies, of which the most common anomalies were albinism (1.6%) and microcephaly (0.7%). These data provide a baseline estimate of the rate of occurrence of developmental anomalies and/or mutations in a killifish population from a relatively pristine estuarine environment.

The Northern subspecies of killifish, *Fundulus heteroclitus macrolepidotus*, spawn in Maine in estuaries in June and July during daily high tides[1,2]. The adults may migrate to and from full strength seawater (SW, ~30 ppt) to freshwater (<1 ppt) but tend to spawn in brackish water (~10 ppt)[1,2]. As the tide ebbs, some embryos remain immersed and some embryos become stranded on rocks and vegetation. These stranded embryos are exposed to air for long periods (up to 14 days)[1]. In spite of enduring significant transient desiccation and thermal stress, aerially incubated embryos develop normally and hatch when flooded by high tides after 12-14 days[1,2]. During our ongoing studies on the physiological and molecular mechanisms these embryos employ to resist desiccation stress[1] we noticed that there were a number of developmental abnormalities and/or mutants that appeared in our cultures. Northeast Creek on Mount Desert Island, ME is considered a relatively pristine environment, and animals from this population have been used for a variety of physiological studies as well as for genomic analyses. We felt a preliminary survey of the occurrences and types of embryo anomalies or mutations that spontaneously occur in this population would provide useful baseline information for research, particularly for investigations of embryonic mutations resulting from exposure to environmental pollutants.

Fish were caught in minnow traps at Northeast Creek and kept in aquaria with natural running SW (~30 ppt). Gametes were gently expressed from fish into a beaker with 25 ml of 10 ppt artificial seawater (ASW; Instant Ocean, Mentor, OH). For these experiments 10 ppt ASW was used; as it approximated the salinity at the sites in the estuary at which fish spawn. After 30 min, the embryos were rinsed with 10 ppt ASW, placed on filter paper moistened with 10 ppt ASW in Petri dishes, and cultured aerially in a chamber in which the humidity was equilibrated to that of 10 ppt ASW[1]. Embryos from 7 days post-fertilization (dpf) to 14 dpf were inspected daily for anomalies using a dissecting microscope. Anomalous embryos were classified, based on deformation or alteration of normal embryo body morphology. Typical examples were photographed, and an extensive reference file of the number of types of anomalies was established.

In total, 13667 fertilized embryos were examined from 11 separate batches. The average number of males and females (mean ± S.E.) used per batch was 7 ± 3 and 13 ± 5. Twenty-six individual types of morphological anomalies were identified. The overall mutation/anomaly rate was about 6%. The six most frequent anomalies were (occurrence rate shown in parentheses): albino (1.6%), severe head and body deformation (0.8%), microcephaly (0.7%), only chromatophores but no body development (0.5%), microcephaly and missing tail (0.2%) and reduced coloration with scattered chromatophores (0.2%). A number of rare anomalies such as two-headed embryos (0.07%) were also noted. In general the types of anomalies noted also have been observed in zebrafish and other species. This preliminary survey provides valuable initial baseline data that characterize embryonic development anomalies and possible mutations in the Northeast Creek killifish population.

Brent Lawson was supported by NSF REU (NSF DBI-1005003) and Ari Dehn by NIH/NIGMS Maine IDeA Network for Biomedical Research Excellence fellowship (P20GM103423).

1. **Chuaypanang S, Kidder GW, Preston RL.** Desiccation resistance in embryos of the killifish, *Fundulus heteroclitus*: Single embryo measurements. *J. Exp. Zool.* 319A: 179-201, 2013.
2. **Petersen, CW, Salinas, S, Preston, RL, Kidder III, GW**. Spawning periodicity and reproductive behavior of *Fundulus heteroclitus* in a New England salt marsh. *Copeia* 2010: 203-210, 2010.